NEAR-SURFACE NON-CONDENSABLE GAS ENRICHMENT IN THE MARTIAN POLAR REGIONS FROM MCS SURFACE OBSERVATIONS.

S. Piqueux[1], A. Kleinböhl[1], P. Hayne[1], D. Kass[1], J. Schofield[1], D. McCleese[1], M. Richardson[2], [1]*Jet Propulsion Laboratory, California Institute of Technology, Pasadena, California, USA (Sylvain.Piqueux@jpl.nasa.gov),* [2] *Aeolis Research, Pasadena, California, USA.*

Introduction: A significant fraction of the Martian atmosphere condenses on the surface in the polar regions during the local Fall and Winter. As a result, the volumic mixing ratio of non-condensable gases, i.e. Ar (~1.9%), N_2 (~1.9%), O_2 (~0.1%), and CO (~0.1%) [1] is expected to increase as a function of season and latitude [2,3,4,19]. Observations have confirmed this depletion [5,6], at least in the South. The low brightness temperatures of CO_2 ice noticed in places may also be an expression of non-condensable gas enrichment near the surface [7,8,9]. As the non-condensable gases are enriched, the partial pressure of CO_2 decreases. The decrease in partial pressure results in a decrease in equilibrium condensation temperature for the surface frosts.

Here, we present an analysis of North and South CO_2 seasonal caps surface temperature observations by the Mars Climate Sounder (MCS) [10,11] onboard the Mars Reconnaissance Orbiter. In the South, we show that ground temperatures associated with frozen surfaces are ~0-4 K lower than anticipated, with latitudinal and seasonal trends generally in phase with the growth and retreat of the seasonal polar cap. Near-surface non-condensable gas mixing ratios implied by these low measurements approaches ~50%, close to modeled values [2,3,4,19], but larger than measured for the entire atmospheric column (e.g., ~20% [5,6]). In the North, a deep depletion is observed near the pole (0-5K, equivalent to <50% CO_2), but with a transient increase near the peak of the polar night (near *Ls*~270).

Methodology: To quantify the depletion of atmospheric CO_2 gas in the polar regions, we compare the temperature of the CO_2 seasonal caps with a prediction of the local frost point temperature (T_{CO2}) assuming a non-depleted atmosphere. The theoretical local frost point T_{CO2} is determined using MOLA topography and season (to calculate the local atmospheric pressure [12]) in conjunction with Clausius Clapeyron's law [13].

The kinetic temperature of CO_2 ice (T_k) is not accessible from remote surface temperature measurements with a single wavelength, but multispectral observations can be used to characterize the surface emissivity, and derive the kinetic temperature T_k of CO_2 ice. We use MCS atmospherically-corrected surface brightness temperatures observations [11,15] acquired at multiple wavelengths to derive the emissivity of the surface (itself controlled by the equivalent crystal sizes *d* [7,14]) and then access the kinetic temperature of the surface CO_2 ice T_k. To do so, we derive the mathematical solution for $\{T_k;d\}$ satisfying surface temperatures observations T_{16} and T_{12} (MCS channels A1 and A4). In other words, we solve for *Eq. 1*, which is a system of two equations linking two unknown (T_k and *d*), with two measurements (T_{16} and T_{12}).

$$\{T_k;d\} <=> \begin{Bmatrix} T_{16} = f(T_k;\varepsilon_{16} \equiv d) \\ T_{12} = f(T_k;\varepsilon_{12} \equiv d) \end{Bmatrix} \quad (1)$$

In *Eq. 1*, *f* is a function obtained from modeling (*Fig. 1*), and linking CO_2 ice emissivity with crystal size and wavelength. *Fig. 1* assumes no surface dust or water ice contamination, such that the emissivity ε of CO_2 ice crystals is only a function *f* of the crystal size *d* [7,15,16].

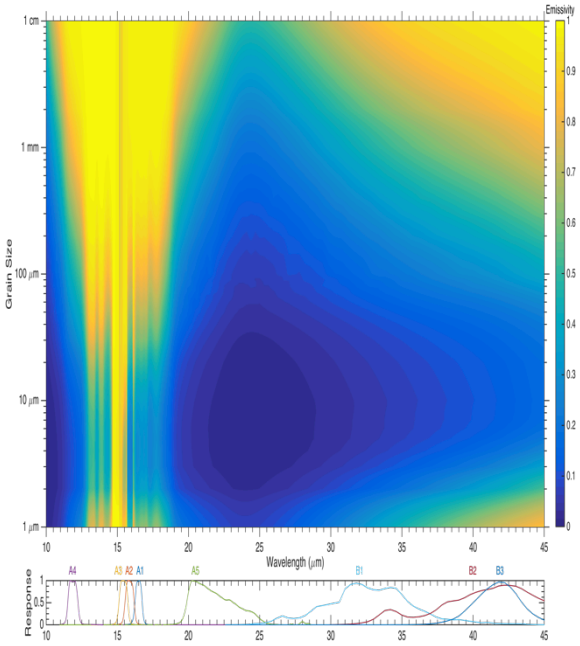

Figure 1: *Modeled emissivity for CO_2 ice as a function of crystal size and wavelength. MCS channels are indicated at the bottom. Modified from [15].*

We favor T_{16} and T_{12} over other measurements because the emissivity of CO_2 ice at these wavelengths is least sensitive to the crystal size *d*, and closest to T_k. We note that T_{15} (A3) and $T_{15.5}$ (A2) have significant gaseous CO_2 opacity and are unsuitable for observing the surface. We eliminate low derived emissivity observations (or brightness temperatures) cor-

responding to CO_2 crystal sizes smaller than ~500 µm because they are associated with non unique $\{T_k;d\}$ solutions (*Fig. 1*) that could be confused with micrometer size crytals. Specifically, we eliminate families of observations where $T_{32} < 110$ K corresponding to emissivities $\varepsilon_{32} \sim< 0.35$. Observations matching this criterion are rather uncommon.

Results are presented in terms of temperature difference Δ (*Fig. 2*) between the derived kinetic temperature of CO_2 ice and the predicted local frost point:

$$\Delta = T_{CO2} - T_k \quad (2)$$

Because T_{CO2} accounts for both the seasonal and elevation-driven variations of the local pressure, we assume that Δ is solely a function of the CO_2 depletion in the near surface atmosphere, and ignore surface contaminations and instrumental errors.

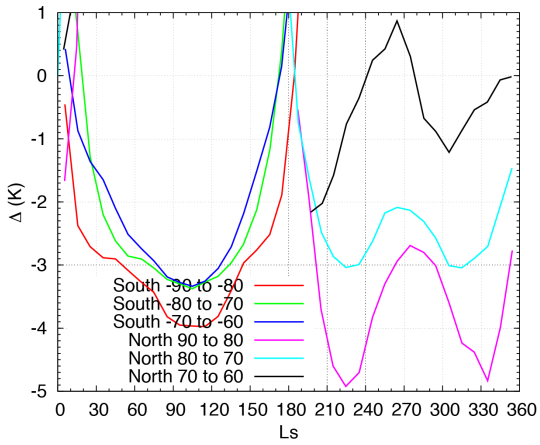

Figure 2: *Evolution of the CO_2 frost point temperature depression with season and latitude. Values above 0 are thought to be a consequence of assuming a fixed scale height.*

Limitations and potential mitigation: There are a number of caveats, limitations and considerations to the approach:

1: T_{CO2} is calculated assuming a fixed atmospheric scale height H (here taken as 9 km). [12] has shown that H varies locally and seasonally, hence impacting the local pressure and therefore Δ. Future work will incorporate a space- and time-dependent estimation of H constrained by MCS retrievals and circulation modeling. The use of the fixed scale height implies that the relative Δ difference between the North and the South may not be meaningful. At the workshop, we will present an analysis using a better estimation of the scale height;

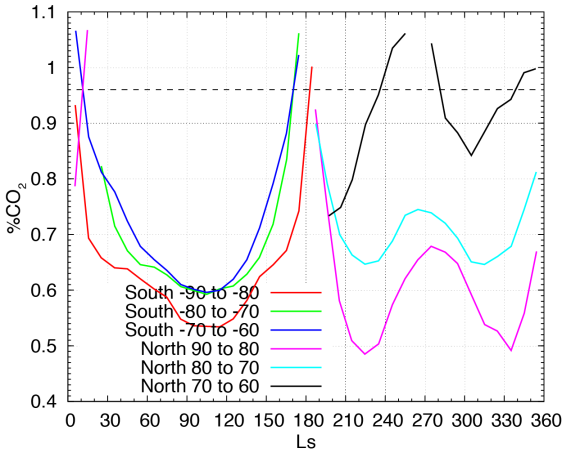

Figure 3: *Evolution of the CO_2 mixing ratio (called here %CO_2) with season and latitude. Values above 1. are thought to be a consequence of assuming a fixed scale height.*

2: Solving for *Eq. 1* assumes no dust and water ice contamination on the surface. While the validity of this assumption is debatable in the polar night, springtime jetting activity on the ice brings dust on the cap that partially masks the spectral properties of CO_2 ice and yields a diurnal temperature cycle [17,18]. For this reason, the technique presented here cannot be used at times and in regions where jetting activity occurs (e.g., no usable data in the North at $0<Ls<70$, and $Ls>200$ in the South).

3: The proposed approach requires the presence of surface CO_2 ice, and is therefore limited to the polar regions. Future work will explore the possibility to leverage the presence of diurnal CO_2 frost to expand this work at nearly all latitudes, even though little to no depletion is generally expected beyond the poles.

Results: The evolution of Δ (and equivalent mixing ratio) versus season and latitude band is presented in *Fig. 2* and *Fig. 3* and shows in the South:

- a decrease of the frost point temperature from the early Fall (Ls~0) to Ls~110, which corresponds to the time of the maximum extent of the cap [15]. This timing is consistent with GRS observations [5,6] but less so with the GCM results of [3,4] where the peak depletion is predicted near Ls~150. We Note that [19] predicts the peak depletion at Ls~110;
- the CO_2 depletion generally increases towards the pole in agreement with GRS observation [5,6], and we note that mapping (*Fig. 4*) indicates that the peak depletion occurs a few degrees off the geographic pole, in correlation with the offset of the perennial CO_2 cap;

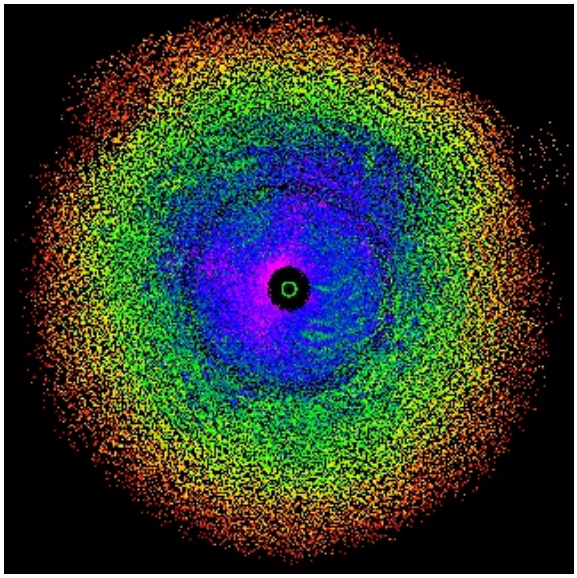

Figure 4: *Map of the CO_2 frost point depression derived from 29<MY<33 data around the South Pole of Mars (-90° to -50°N), at 90<Ls<120. Red: No depletion; Purple: 5K depletion (equivalent to ~50% CO_2 and ~50% non condensables).*

- the evolution of the CO_2 depletion does not follow the monotonic pace of the growth and retreat of the cap, but instead follows periods of accelerations generally when the cap is growing (e.g., 0<*Ls*<50), of pause (e.g., 50<*Ls*<60) and reduction of the depletion, generally when the cap is retreating (e.g., 110<*Ls*<200);

In contrast, in the North, we find:

- a decrease of the frost point temperature from the early Fall *(Ls*~180) to *Ls*~220, which corresponds to a phase of seasonal cap growth [15]. Between *Ls*~220 and *Ls*~280, the depletion decreases, while the cap continues its growth, possibly indicating an injection of non-depleted atmosphere into the polar vortex. The trend is symmetrical after *Ls*~280, with a re-decrease of the mixing ratio of CO_2 gas, and the final decrease until the cap disappears past *Ls*~20.
- These observations contrasts with published work using GRS observations [5,6] indicating no clear non-condensable enrichment near the North Pole, as well as eith GCM simulations [3,4]. They are consistent with the modeling results of [2].

Discussion: The kinetic surface temperatures derived from MCS measurements provide a clear signal into the local enrichment of the atmosphere with non-condensable species due to the condensation of CO_2. This will allow us to map and characterize the relationship between the atmosphere and the surface in the Martian polar night.

In the North, the complex depletion pattern induced by the evolution of Δ suggests an injection of atmospheric gas from outside the polar vortex. This permeability of the North polar vortex contrasts with the observations in the South suggesting a significant enrichment near the surface in non-condensable gases reaching up to ~50% at *Ls*~110. Maintaining both this latitudinal and vertical gradient is challenging because of the density gradient induced by this depletion [3,4] and other mixing processes [19].

The lowering of the kinetic temperature of CO_2 ice reduces the ability of CO_2 ice to efficiently radiate heat in the winter, might have an impact on the mass budget of the seasonal caps, and can help us constrain the general circulation.

Ongoing work will further refine these results and mitigate some of the above limitations. It will also further explore the implications for the inferred enrichments.

Nomenclature: T_k: kinetic temperature of seasonal CO_2 ice; T_{CO2}: predicted kinetic temperature of CO_2 ice assuming no enrichment by non-condensable gases; *d*: surface seasonal CO_2 ice crystal size; T_n where *n* is an integer: brightness temperature at *n* μm; ε_n where *n* is an integer: emissivity derived at *n* μm; *H*: Atmospheric scale height (9 km in this work).

Acknowledgements: This work was performed at the Jet Propulsion Laboratory, California Institute of Technology, under a contract with NASA. Support by the Mars Climate Sounder Mars Reconnaissance Orbiter Project acknowledged.

References: [1] Mahaffy et al., 2013, *Science*, 341,6143,263-266; [2] Noguchi, K., Ikeda, S., Kuroda, T., Tellmann, S., Patzold, M., 2014, *J. Geophys. Res.*, 119, 12, 2510-2521; [3] Forget, F., Millour, E., Montabone, L., Lefebre, F., 2008, *3rd Mars Atmosphere: Modeling and Observations*, #9106; [4] Forget, F., Montabone, L., Lebonnois, S., 2004, *2nd Mars Atmosphere: Modeling and Observations*, #Forget4; [5] Sprague et al., 2004, *Science*, 306, 1364-1367; [6] Sprague et al., 2012, *J. Geophys. Res.*, 117, E04005; [7] Hayne et al., 2012, *J. Geophys. Res.*, 117, E08014; [8] Kieffer et al., 1976, *Science*, 193, 780-786; [9] Kieffer et al., 1977, *J. Geophys. Res.*, 82(28), 4249-4291; [10] McCleese et al., 2007, *J. Geophys. Res.*,112, E05S06; [11] Kleinböhl et al., 2009, *J. Geophys. Res.*,114, E10006; [12] Withers, P., 2012, *Space Sci. Rev.*, 170, 837-860; [13] James, P., Kieffer, H., Paige, D., 1992, *Mars*, Univ. of Arizona Press; 934-968; [14] Kieffer, H., Titus, T., Mullins, K., Christensen, P., 2000, *J. Geophys. Res.*, 105, E4, 9653-969; [15] Piqueux et al., 2016, *J. Geophys Res.*, 121, 1174-1189; [16] Hansen, G., 1997, *J. Geophys. Res.*, 102, E9, 21,569-21,58; [17] Kieffer, H., 2007, *J. Geophys. Res.*, 112, E08005; [18] Pilorget et al., 2013, *J. Geophys. Res.*, 118, 2520–2536; [19] Lian, Y., et al., 2012, Icarus, 218, 1043–1070.